Structure Functions and Particle Production in the Cumulative Region: two different exponentials *

M.Braun and V.Vechernin
Department of high-energy physics,
University of S. Petersburg, 198904 S. Petersburg, Russia

Abstract

In the framework of the recently proposed QCD based parton model for the cumulative phenomena in the interactions with nuclei two mechanisms for particle production, direct and spectator ones, are analysed. It is shown that due to final state interactions the leading terms of the direct mechanism contribution are cancelled and the spectator mechanism is the dominant one. It leads to a smaller slope of the cumulative particle production rates compared to the slope of the nuclear structure function in the cumulative region $x > 1$, in agreement with the recent experimental data.

1 Introduction

We have recently proposed a QCD based parton model for the cumulative phenomena in the interactions with nuclei [1]. In the model quark diagrams are summed in the vicinity of all intermediate thresholds at which some quarks of the nucleus ("donors") transfer all their longitudinal momenta to the distinguished active quark and become soft. Particle production proceeds in the model via two different mechanisms, the direct and spectator ones, schematically shown in Fig. 1 $a, b.$, respectively. The simpler direct mechanism leads to the same x dependence of the production rate I_d as for the structure function $F_2(x)$ in the region $x > 1$. It is roughly an exponential in x

$$I_d(x) \sim F_2(x) \sim \exp(-b_0 x) \tag{1}$$

where the slope b_0 is determined by the QCD coupling constant and quark mass. The spectator mechanism besides involves interactions between partons of the projectile and target nucleus. It was shown in [1] that each donor quark has to interact with the projectile.

*Supported by the Russian Foundation for Fundamental Research, Grant No. 94-02-06024-a

As a result the spectator contribution I_s also behaves in x as an exponential but with a different slope

$$I_s(x) \sim \exp(-b_s x) \tag{2}$$

the slope b_s depending not only on the QCD coupling constant and quark mass but also on the partonic amplitude. With a particular parametrization for the latter chosen in [1] the slope b_s was found to be somewhat larger than b_0, so that the spectator contribution resulted smaller than the direct one. Then the total particle production rate behaves in x exactly as the structure function. At the time when the paper [1] was written there existed no reliable data on the cumulative structure functions except the old data on the deuterium at low energies and not really in the deep inelastic region [2]. These deuterium data had the slope in x much steeper than particle production data from [3,4]. Assuming the direct mechanism for particle production this resulted in very different values for the effective coupling constant found in [1] for the two cumulative phenomena. In view of a preliminary character of the deuterium data we preferred not to pursue this point any further in [1].

However recently a new set of data on the structure function of ^{12}C in the region $0.8 \leq x \leq 1.3$ was published [5], which essentially agrees with the x dependence observed on the deuterium in [2]. Thus it seems to be confirmed that the structure function and particle production have different x dependence in the cumulative region. The slope b_0 as observed in [2] and [5] is roughly 16, whereas the slope b_p of the particle production rate is of the order $6 \div 8$ [3,4].

This circumstance gives us a motivation to reconsider our study of the cumulative phenomena in the light of the experimental evidence for two different exponentials for the structure function and particle production. In the framework of our model it means that it is the spectator mechanism that gives the bulk of particle production.

In this note we first demonstrate that final state interactions, not taken into account in [1], cancel the leading terms in the direct contribution, so that it becomes much less than the spectator one. Then particle production in the cumulative region indeed goes predominantly via the spectator mechanism. To be able to explain the experimental slope we study a wider class of parametrizations for the partonic amplitude than in [1]. The spectator slope b_s results very sensitive to the magnitude of the hadronic diffractive cross-sections. The parametrization used in [1], which lead to a rather large value for $b_s \sim 15$, corresponded to a zero diffractive cross-section. Raising the ratio of the diffractive to elastic cross-section up to 1.5 results in lowering b_s down to $7 \div 9$, not very far from the experimentally observed value $6 \div 8$. However it does not seem possible to push b_s still further down without entering into a serious conflict with the data on hadronic cross-sections.

Note that a more phenomenological attempt to explain smaller slopes for the cumulative particle production is made in [6], where the existence of multiquark clusters in the nucleus and their properties are postulated and the quark-gluon string model formalism of [7] is used to calculate production rates.

The paper is organized as follows. In Sec. 2 we show how the leading terms in the direct contribution are cancelled by final state interactions. In Sec. 3 the partonic amplitude is related to the hadronic one and the data on hadronic cross-sections are used to study

its possible parametrizations. In Sec. 4 we calculate the particle production rate by the spectator mechanism and compare its x dependence to that of the structure function and the experimentally observed one.

2 Cancellation of the direct contribution

In the upper blob of Fig. 1 *a* the inclusive cross-section off the active quark enters in the triple Regge kinematical region, since the scaling variable x of the produced particle should be as close as possible to that of the active quark. Therefore we can redraw the diagram of Fig. 1 *a* in the form shown in Fig. 2 *a*. However we have also to take into account final state interactions of the produced particle with donor quarks which raise its longitudinal momentum. An example of these is shown in Fig. 2 *b*. The diagrams of Fig. 2 *a* and *b* are not the only ones which give contribution. In fact taking a diagram with a certain pattern of interactions with donor quarks one should sum over all places where the two upper reggeons from the triple Regge interaction are attached to the active quark. We are going to demonstrate that this sum vanishes in the limit when the donor quarks loose all their longitudinal momentum.

Let the number of donors be n. We denote the momenta of the left active quark $\kappa_0, ...\kappa_l$ before the interaction with the reggeon and $\kappa'_l, \kappa'_{l+1}...\kappa'_n \equiv \kappa$ after this interaction. Analogous quantities on the right side hereafter will be labelled with tildas (see Fig. 2 *a, b*). We use the light-cone variables $k = (k_+, k_\perp)$. The donor quarks lie on the mass shell between the interactions. So there minus momenta ("energies") take on physical values

$$k_{i-} = (m^2 - k_{i\perp}^2)/2k_{i+} \equiv \mu_i \tag{3}$$

From energy conservation we find for the energies of the active quark

$$\kappa_{i-} = Np_{1-} - \sum_{n+1}^{N-1} \mu_j - \sum_{1}^{i} \mu_j - \sum_{i+1}^{n} k_{j-}^{(0)}, \quad i = 1, 2, ...l \tag{4}$$

and

$$\kappa'_{i-} = \kappa_- + \sum_{i+1}^{n} (\mu_j - k_{j-}^{(0)}) \quad i = l, l+1, ...n-1 \tag{5}$$

where N is the total number of partons in the nucleus and $k_i^{(0)}$ are the momenta of the left donors before the interaction. Integrations over $k_{i-}^{(0)}$ can then be done easily, since all singularities coming from the active quark propagators lie on the opposite side of the real axis as compared to the donor propagators. As a result $k_{i-}^{(0)}$ are substituted by $\mu_i^{(0)}$ in (4) and (5). In the limit when the donor quarks loose all there longitudinal momenta μ_i become large and from (4) and (5) one obtains for the ith active quark propagator

$$1/\sum_{1}^{i} \mu_j, \quad i = 1, 2, ...l \tag{6}$$

and

$$-1/\sum_{i+1}^{n}\mu_j, \quad i=l,l+1,...n-1 \tag{7}$$

Now we pass to the triple Regge interaction. The momentum of the upper left reggeon q is

$$q=\kappa_l'-\kappa_l \tag{8}$$

So $q_-=\sum_1^n\mu_i$. Calculating q_+ and $q_\perp$ we find

$$q^2=-2p_{1+}(\Delta-\sum_1^n x_i)\sum_1^n\mu_i+(\kappa+\sum_1^{N-1}k_i)_\perp^2 \tag{9}$$

Here x_i are the scaling momenta of the donors after the interactions, $x_i\to 0$; $\Delta=n+1-x$ where x is the scaling variable of the produced particle. All scaling variables are defined here relative to the average longitudinal momentum of the initial quarks of the nucleus. They are three times larger than the standard ones defined relative to the nucleon momentum. At the threshold $\Delta\to 0$. The important thing about (9) is that q^2 does not depend on l, that is, on the place at which the reggeon is attached.

However there still remains some dependence on l in the energy on which the upper reggeons depend. In fact the factor corresponding to the triple Regge interaction is given by

$$g(t)(s_l\tilde{s}_{\tilde{l}})^{\alpha(t)}(M^2)^{\alpha(0)-2\alpha(t)}, \quad t=q^2 \tag{10}$$

Here q^2 is given by Eq. (9), $g(t)$ is the three-reggeon vertex, $M^2=(\Delta-\sum_1^n x_i)s$ where s is the standard energy variable; $s_l=\xi_l s$ where ξ_l is the scaling variable of the left active quark at the moment of its interaction with the reggeon and $\tilde{s}_{\tilde{l}}$ is a similar quantity on the right. All the three reggeons are taken to be pomerons with the trajectory $\alpha(t)$. We have also to take into account that the lth propagator of the active quark is splitted into two by the interaction with the reggeon, which results in an extra factor $1/\xi_l$. Introducing it into (10) we finally obtain for the triple Regge interaction factor

$$g(t)s^{\alpha(0)}(\xi_l\tilde{\xi}_{\tilde{l}})^{\alpha(t)-1}(\Delta-\sum_1^n x_i)^{\alpha(0)-2\alpha(t)} \tag{11}$$

If we assume weak (logarithmic) dependence of the cross-section on energy then we have to take for the effective pomeron intercept $\alpha(0)=1$. Then the dependence of the expression (11) on l and $\tilde{l}$ is also weak (it enters only through the term $\xi_l^{\alpha' t}$ with small α' and t). Neglecting this dependence we find that the triple Regge interaction factor does not depend on the place where it is attached and is common to all the diagrams of the type shown in Fig. 2.

Then we have only to sum various diagrams forgetting about the common triple Regge factor. Diagrams with different l (or/and $\tilde{l}$) differ only by their active quark propagators.

For a given l the factor coming from the left active quark propagators is found from (7) and (8) to be

$$\prod_{i=1}^{l}(1/\sum_{1}^{i}\mu_j)\prod_{i=l}^{n-1}(-1/\sum_{i+1}^{n}\mu_j) \tag{12}$$

Upon symmetrizing in the soft donors it becomes

$$(l!(n-l)!)^{-1}(-1)^{n-l}\prod_{1}^{n}1/\mu_i \tag{13}$$

The sum of (13) over all $l = 0, 1, ...n$ evidently gives zero. Thus in the described approximation when the slow change of the triple reggeon interaction with the energy of the active quark is neglected all the diagrams of the type shown in Fig. 2 cancel in the sum.

3 Parton interaction and hadronic cross-sections

With the bulk of the direct contribution cancelled, particle production in the cumulative region goes predominantly via the spectator mechanism of Fig. 1 *b*. It involves interactions between partons of the projectile and donors from the nucleus, characterized by the partonic amplitude a. We normalize it according to

$$2\mathrm{Im}\, a(0) = \sigma \tag{14}$$

where $a(0)$ is the forward amplitude and σ is the partonic cross-section. As shown in [1] each donor parton has to take part in the interaction with the projectile. With n donors, this gives a factor a^n which is responsible for the difference between the slopes of the structure function and particle production. The parametrization of a and its magnitude thus aquire the decisive role in describing the experimental slope.

Of course, a is not the quantity to be directly measured experimentally. It can however be related to the data through hadronic (pp or $p\bar{p}$) interaction [8]. The elastic hadronic amplitude can be represented through partonic interaction as shown in the diagram of Fig. 3. Taking the c.m. system one finds that the longitudinal components $q_{i\pm}$ of the transferred momenta are small. Also the upper part of the diagram belonging to the projectile does not depend on q_{i+} and the lower, target part does not depend on q_{i-}. Integrating over $q_{i\pm}$ one then finds that for a diagram with n interactions, M partons in the projectile and N ones in the target the amplitude is given by

$$iA_n^{(M,N)}(q_\perp) = n!C_M^nC_N^n\int\prod_{1}^{n}(\frac{d^2q_{i\perp}}{(2\pi)^2}ia(q_{i\perp}))(2\pi)^2\delta^2(q-\sum_{1}^{n}q_i)F_n^{(M)}(q_{i\perp})F_n^{(N)}(q_{i\perp}) \tag{15}$$

Here $F_n^{(M,N)}(q_{i\perp})$ are the n-fold transverse form-factors for the projectile (M) and target (N). Their Fourier transforms give parton distributions in the transverse space $F_n^{(M,N)}(b_i)$. The amplitude (15) thus can be presented as an integral in the transverse space

$$iA_n^{(M,N)}(q_\perp) = n!C_M^nC_N^n\int d^2B\exp(iqB)\prod_{1}^{n}(d^2b_id^2b_i'a(B-b_i+b_i'))F_n^{(M)}(b_i)F_n^{(N)}(b_i') \tag{16}$$

This is only a contribution from given numbers of partons in the projectile and target. Summing over M and N we obtain for the elastic amplitude with n partonic interactions

$$iA_n(q_\perp) = (1/n!) \int d^2B \exp(iqB) \prod_1^n (d^2b_i d^2b'_i a(B - b_i + b'_i)) F_n(b_i) F_n(b'_i) \tag{17}$$

where for the projectile

$$F_n(b_i) = \sum_{M \geq n} (M!/(M-n)!) F_n^{(M)}(b_i) \tag{18}$$

and similarly for the target.

To move further one has to make some assumptions about the multiparton distributions $F_n(b_i)$. The simplest one is to assume that partons are completely independent: their number is distributed according to Poisson's law and multiparton distributions factorize. One then obtains

$$F_n(b_1, ...b_n) = \nu^n \prod_1^n \rho(b_i) \tag{19}$$

where ν is the mean number of partons in the projectile or target and the one parton distribution ρ is normalized to unity

$$\int d^2b \rho(b) = 1 \tag{20}$$

Putting (19) into (17) and summing over n one arrives at an eikonal amplitude

$$iA(q_\perp) = \int d^2B \exp(iqB)(\exp(ip(B)) - 1) \tag{21}$$

where the eikonal factor is

$$p(B) = \nu_p \nu_t \int d^2b d^2b' \rho_p(b) \rho_t(b') a(B - b + b') \tag{22}$$

and the subscripts p and t refer to the projectile and target, respectively. This form of the amplitude coincides with the one found in the multipomeron exchange model with factorizable vertices [9]. Eq. (22) then gives the contribution of a single pomeron exchange.

One commonly assumes that both ρ and a have a Gaussian dependence on the impact parameter:

$$\rho_{p,t}(r) = (1/\pi r_{p,t}^2) \exp(-r^2/r_{p,t}^2), \quad a(r) = (i\sigma/2\pi r_0^2) \exp(-r^2/r_0^2) \tag{23}$$

where we have taken a pure imaginary, for simplicity. Then one easily finds simple expressions for the eikonal factor, the hadronic total, elastic and inelastic cross-sections and also for the slope of the elastic cross-section B^{el}:

$$p(B) = ix \exp(-B^2/R^2)$$

$$\sigma^{tot} = 2\pi R^2 \phi_1(x)$$
$$\sigma^{el} = \pi R^2 (2\phi_1(x) - \phi_1(2x))$$
$$\sigma^{in} = \pi R^2 \phi_1(2x)$$
$$B^{el} = (R^2/2)\phi_2(x)/\phi_1(x) \tag{24}$$

where $R^2 = r_p^2 + r_t^2 + r_0^2$ is the total interaction radius squared, $x = \nu_p \nu_t \sigma/(2\pi R^2)$ and the functions $\phi_{1,2}(x)$ are defined by

$$\phi_n(x) = \sum_{k=1}^{\infty} (-1)^{k-1} x^k/(k! k^n) \tag{25}$$

Taking the ratio of any pair of the quantities in (24) and comparing it to its experimental value one can determine x. Then one of Eqs. (24) can be used to find R^2. With x and R^2 determined, the cross-section $\nu_p \nu_t \sigma$ can be found. Values of r_p and r_t are more or less known from electromagnetic properties of the projectile and target, thus r_0 can also be found. So, in the end, the only parameters left are the average numbers of partons in the projectile and target ν_p and ν_t. At low energies the valence quark approximation seems to be good enough, which implies $\nu_p = \nu_t = 3$ for pp or $p\bar{p}$ interactions.

This standard procedure was used in [1] to determine the parameters entering the spectator mechanism. As mentioned, it lead to a relatively small a, so that the slope of the spectator spectrum resulted even steeper than that of the structure function. However, apart from this unsatisfactory result for cumulative production, the discussed parametrization has a more fundamental (and well-known) defect. As one can deduce from the first three equations in (24) it gives no diffraction. This property of the pure eikonal amplitude can be easily understood in the framework of the Gribov approach to multiple scattering [10], where it corresponds to retaining only the initial particle state in the sum over all intermediate states. A possible remedy consists in changing the eikonal amplitude (21) by the quasi-eikonal one with a diffraction factor $\xi > 1$ [11]:

$$iA(q_\perp) = \int d^2B \exp(iqB) \xi^{-1} (\exp(i\xi p(B)) - 1) \tag{26}$$

With this factor Eqs. (24) change as follows

$$\sigma^{tot} = \xi^{-1} 2\pi R^2 \phi_1(x)$$
$$\sigma^{el} = \xi^{-2} \pi R^2 (2\phi_1(x) - \phi_1(2x))$$
$$\sigma^{in} = \xi^{-1} \pi R^2 \phi_1(2x) \tag{27}$$

and B^{el} does not change at all. From (27) one finds the diffractive cross-section

$$\sigma^{dif} = (\xi - 1)\sigma^{el} \tag{28}$$

so that the new parameter ξ can be directly taken from experiment.

In our partonic approach the quasi-eikonal parametrization (26) means that instead of (19) we take

$$F_n(b_1, ...b_n) = \xi^{(n-1)/2} \nu^n \prod_1^n \rho(b_i) \tag{29}$$

both for the target and projectile.

The quasi-eikonal parametrization leads to values of a considerably larger than without diffraction because of a stronger screening effect introduced by diffractive states (see Table). For the maximum value of $\xi \simeq 2.4$ compatible with the experimental data at $\sqrt{s} = 23.5\ GeV$ it leads to the value of the corresponding parton-nucleon cross-section σ_1 nearly three times larger than with $\xi = 1$ used in [1]. Note that the absolute value of σ_1 then results quite large ($\sim 50\ mb$). It is interesting that values of σ_1 of a similar order are also favoured by the study of the behaviour of the nuclear structure functions in the opposite kinematical region at small x [12]. In relation to this we recall that the parton-nucleon cross-section σ_1 is not a directly observable quantity. It only enters hadronic cross-sections as a parameter. The mentioned large value of σ_1 is consistent with all experimental evidence on proton-proton interactions at $\sqrt{s} = 23.5\ GeV$. This large value transforms into the physical value of the pp cross-section as a result of a strong screening effect, that is, because of a highly coherent manner in which the quarks interact.

4 Numerical results and discussion

With the partonic amplitude fixed in the preceding section, one can calculate the spectator contribution to the cumulative production rate, using the coresponding equations from our paper [1] (Eqs. (38), (39) and (41) of [1]), suitably modified to the quasi-eikonal case. We have also corrected a mistake eliminating $p!$ in the denominator of Eq. (39) of [1]. We have chosen the maximum possible value for the diffractive parameter $\xi = 2.4$. Other parameters have been fixed as in [1].

The results of the calculations are shown in Figs. 4 and 5 for the cumulative charged pion production on deuterium and ^{181}Ta, respectively. For comparison the corresponding nuclear structure function $F_2(x)$ at $x > 1$, calculared in [1], is also shown, as well as the available experimental data from [2-5].

One clearly observes that the spectaor mechanism, with a parametrization of the partonic amplitude chosen to account for diffraction, leads to a considerably smaller slope of the production spectra ($b_s \sim 7 \div 9$, see Introduction) compared to the slope of the structure function in the region $x > 1$ ($b_0 \sim 16$), in a good agreement with experimental data.

Thus our model correctly predicts two differents exponential in the cumulative production and in the nuclear structure function at $x > 1$. The difference is due to additional multiple interactions between projectile and target which enter the spectator mechanism for the cumulative production.

References

[1] M.Braun and V.Vechernin, *Nucl. Phys.* **B427** (1994) 614.

[2] W.P.Shüetz *et al., Phys. Rev. Lett.* **38** (1977) 259.

[3] A.M.Baldin *et al., Preprint P1-11168*, (JINR, Dubna, 1977);
A.M.Baldin *et al., Preprint E1-82-472*, (JINR, Dubna, 1982).

[4] N.A.Nikiforov *et al., Phys. Rev.* **C22** (1980) 700.

[5] BCDMS collaboration, *Z. Phys.* **C63** (1994) 29.

[6] A.V.Efremov, A.B.Kaidalov, G.I.Lykasov and N.V.Slavin, *Yad. Fiz.* **57** (1994) 932.

[7] A.B.Kaidalov, *Phys. Lett.* **B116** (1982) 459;
A.B.Kaidalov and K.A.Ter-Martirosyan, *Phys. Lett.* **117** (1982) 247.

[8] M.A.Braun, *Nucl. Phys.* **A523** (1991) 694.

[9] M.S.Dubovikov and K.A.Ter-Martirosyan, *Nucl. Phys.* **B124** (1977) 163;
A.Kaidalov, L.Ponomarev and K.Ter-Martirosyan, *Yad. Fiz.* **44** (1986) 722.

[10] V.N.Gribov, *Zh. Eksp. Teor. Fiz.*, **56** (1969) 892.

[11] A.B.Kaidalov and K.A.Ter-Martirosyan, *Nucl. Phys.* **B75** (1974) 471.

[12] S.J.Brodsky and H.J.Lu, *Phys. Rev. Lett.* **64** (1990) 1342.

[13] N.A.Amos *et al*, *Nucl. Phys.* **B262** (1985) 689.

Table. Cross-sections and elastic slopes for various values of the diffractive factor ξ

ξ	σ^{dif} (mb)	σ_1 (mb)	B^{el} (GeV^{-2})
1.0	0.	16.5	11.1
1.5	3.4	20.2	10.9
2.0	6.8	31.2	10.6
2.2	8.2	44.3	10.6
2.4	9.5	48.3	11.4

Table captions

The first column gives values of the diffractive parameter ξ. In the second column the corresponding pp diffractive cross-section at $\sqrt{s} = 23.5\ GeV$ is shown. In the third column the values of the parton-projectile (proton) cross section are shown, as calculated from Eqs. (24) (from the value of x with $\nu = 3$). The last column shows the resulting elastic slope, its experimental value at $\sqrt{s} = 23.5\ GeV$ being $B^{(el)} = 11.8 \pm 0.30\ GeV^{-2}$ [13].

Figure captions

Fig. 1 Two mechanisms of the cumulative particle production in the parton model, the direct (a) and spectator (b) ones. Dashed and chain lines show gluon and pomeron exchanges, respectively.

Fig. 2 The direct mechanism of the cumulative particle production in the triple Regge approach without (a) and with (b) final state interactions of the produced particle with donor quarks. Shown for the cases ($n = l = \tilde{l} = 2$) and ($n = 2, l = 1, \tilde{l} = 0$), respectively. Notations as in Fig. 1.

Fig. 3 The elastic hadronic amplitude in the parton model. Notations as in Fig. 1.

Fig. 4 $I_D = \frac{xd\sigma}{2dx}(mb)$ is the calculated inclusive cross-section (per nucleon) for cumulative charged pion production on deuteron at $\sqrt{s} = 23.5\ GeV$ (solid curve) and 1800 GeV (dashed one). $F_2^D/2$ is the calculated structure function of the deuteron (per nucleon) for $x > 1$ at $Q^2 = 6\ GeV^2$ (solid curve), 20 GeV^2 (dashed curve) and 500 GeV^2 (short dash curve). $\star$ - the experimental data [2] on the deuteron structure function at $0.8 \leq Q^2 \leq 6\ GeV^2$. The experimental errors are much less than the star symbols and not discernable on our scale.

Fig. 5 $I_A(mb)$ is the same as in Fig. 4 but for the production on ^{181}Ta. Δ - the experimental data [4] on the cumulative charged pion production on ^{181}Ta by 400 GeV incident proton beam. $F_2^A/2$ is the calculated nuclear structure function for the ^{181}Ta at $Q^2 = 50\ GeV^2$ (dashed curve) and ^{12}C at $Q^2 = 100\ GeV^2$ (solid curve). $\Box$ and $\times$ - the experimental data [5] on the ^{12}C structure function at $Q^2 = 61\ GeV^2$ and 150 GeV^2, respectively.

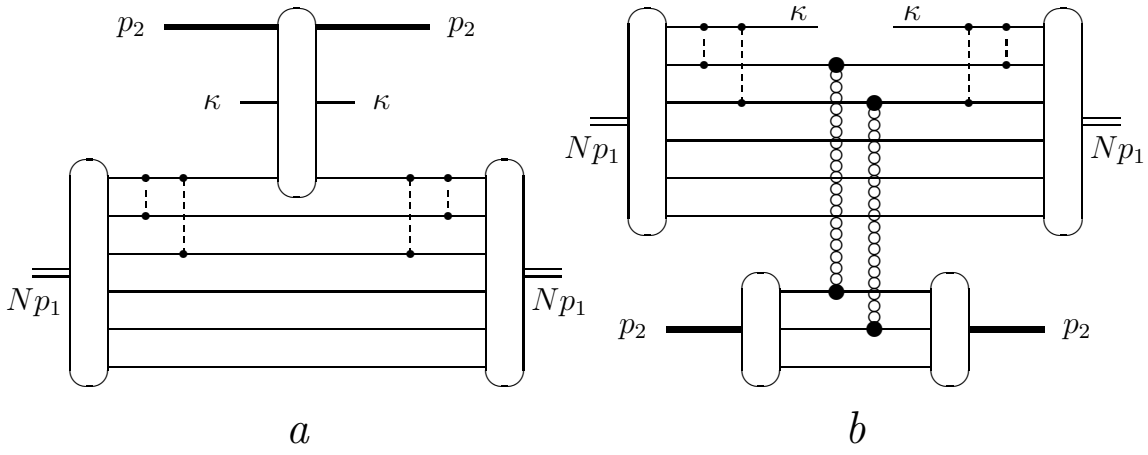

Fig. 1

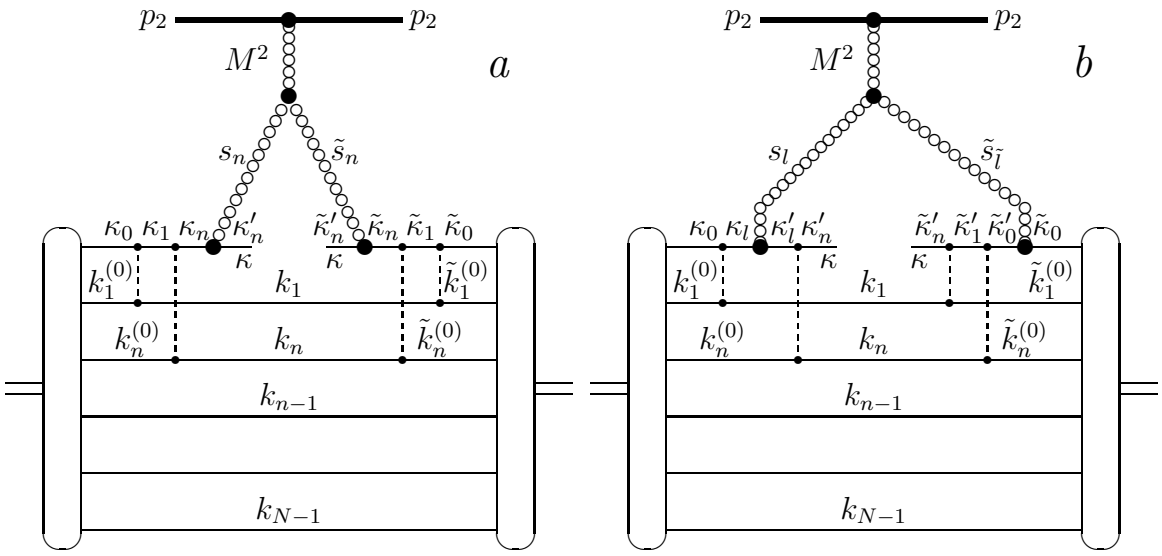
p_2
p_2
M^2
a
s_n
$\tilde{s}_n$
κ_0 κ_1 κ_n κ'_n
κ
$\tilde{\kappa}'_n$ $\tilde{\kappa}_n$ $\tilde{\kappa}_1$ $\tilde{\kappa}_0$
κ
$k_1^{(0)}$
k_1
$\tilde{k}_1^{(0)}$
$k_n^{(0)}$
k_n
$\tilde{k}_n^{(0)}$
k_{n-1}
k_{N-1}
p_2
p_2
M^2
b
s_l
$\tilde{s}_{\tilde{l}}$
κ_0 κ_l κ'_l κ'_n
κ
$\tilde{\kappa}'_n$ $\tilde{\kappa}'_1$ $\tilde{\kappa}'_0$ $\tilde{\kappa}_0$
κ
$k_1^{(0)}$
k_1
$\tilde{k}_1^{(0)}$
$k_n^{(0)}$
k_n
$\tilde{k}_n^{(0)}$
k_{n-1}
k_{N-1}

Fig. 2

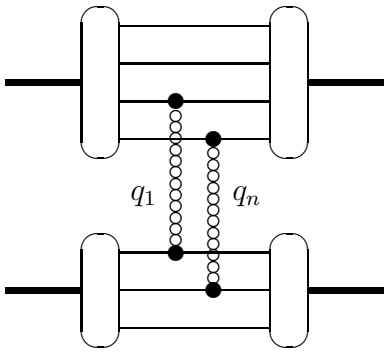
q_1
q_n

Fig. 3

Fig. 4

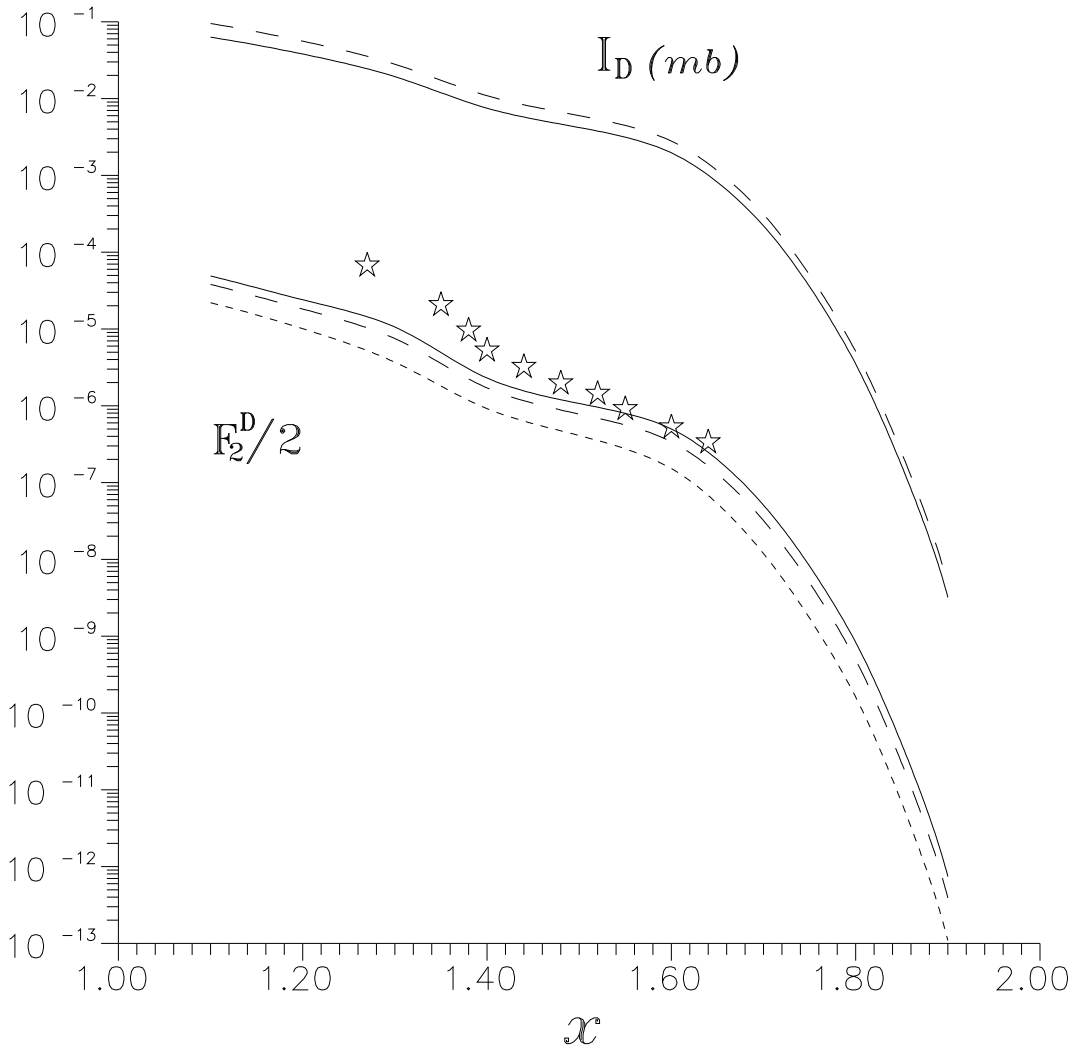
$I_D\ (mb)$
$F_2^D/2$
10^{-1}
10^{-2}
10^{-3}
10^{-4}
10^{-5}
10^{-6}
10^{-7}
10^{-8}
10^{-9}
10^{-10}
10^{-11}
10^{-12}
10^{-13}
1.00
1.20
1.40
1.60
1.80
2.00
x

Fig. 5

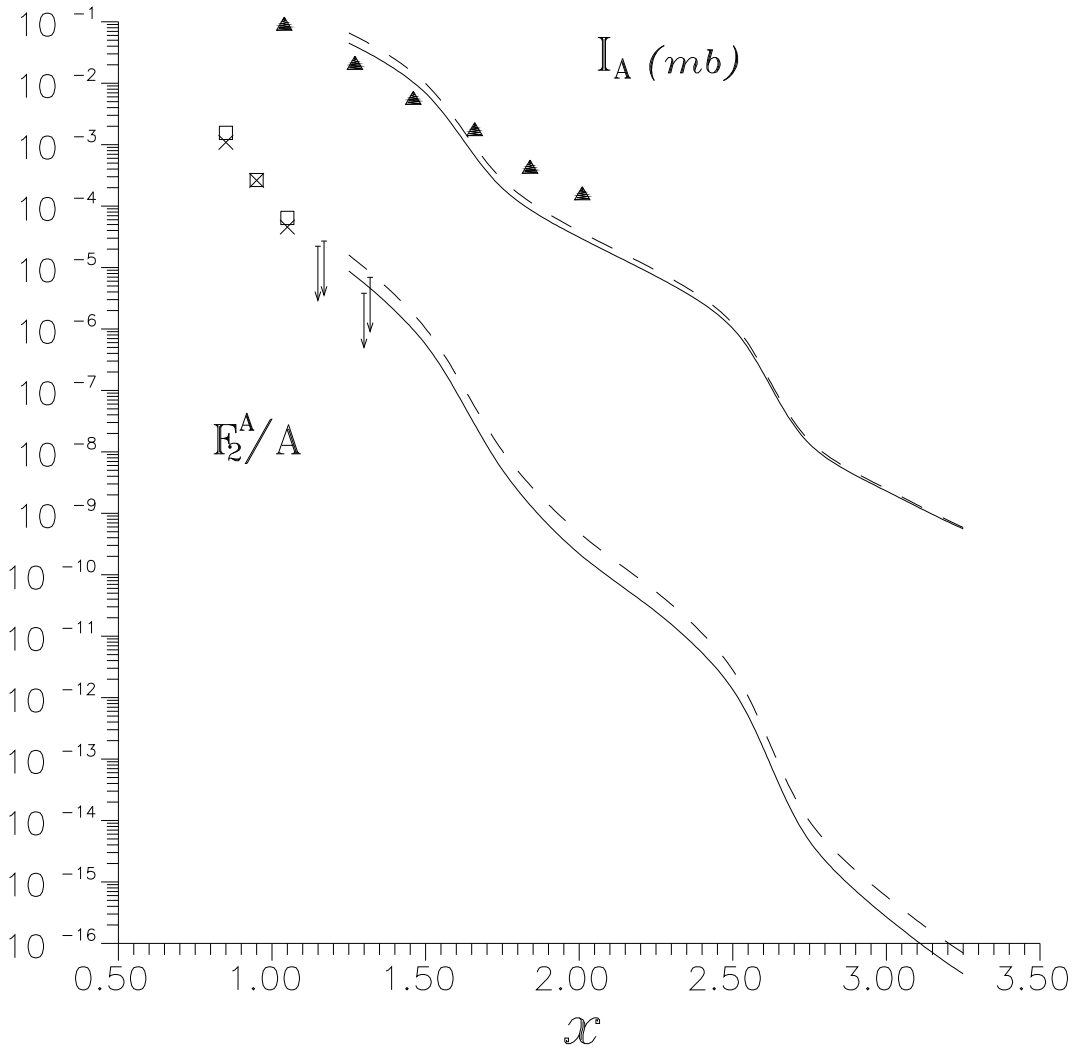
$I_A\ (mb)$
F_2^A/A
10^{-1}
10^{-2}
10^{-3}
10^{-4}
10^{-5}
10^{-6}
10^{-7}
10^{-8}
10^{-9}
10^{-10}
10^{-11}
10^{-12}
10^{-13}
10^{-14}
10^{-15}
10^{-16}
0.50
1.00
1.50
2.00
2.50
3.00
3.50
x